Peak Force Evaluation for an Active Contact Flange

Bernhard Rameder
Institute of Robotics
Johannes Kepler University Linz
4040 Linz
bernhard.rameder@jku.at

Hubert Gattringer
Institute of Robotics
Johannes Kepler University Linz
4040 Linz
hubert.gattringer@jku.at

Andreas Müller
Institute of Robotics
Johannes Kepler University Linz
4040 Linz
a.mueller@jku.at

Ronald Naderer
FerRobotics Compliant Robot Technology GmbH
Johannes Kepler University Linz
4040 Linz
ronald.naderer@ferrobotics.at

Abstract

When employing robots for tasks such as polishing or surface grinding, vibration and peak interaction forces exerted at the robot or the part must be limited. Therefore, such tasks are performed with the help of Active Contact Flanges (ACF). These devices are force controlled and enable fast processing speeds. High contact velocities of the tool result in significant impact forces during interaction with the environment. Consequently, a critical control aspect is the reliable estimation of these forces, which is the focus of this paper. A dynamical model is developed, resulting in a linear time invariant equation of motion, which is solved analytically. Hereby, a homogeneous and a particular solution is derived. The maximum contact force is then determined based on an optimization. Experimental results demonstrate high consistency between measured and calculated contact forces.

1 Introduction

Grinding, polishing and deburring are important tasks in robotics and a key enabler for advanced manufacturing in high wage countries. Due to economic reasons it is important to perform these processes with high speeds. Especially, the contact phase between object and polishing tool on a robot is crucial. Therefore, an Active Contact Flange (ACF) is used to achieve these high speeds, while at the same time impact forces are minimized. These ACFs are mechatronic devices utilizing a double-acting pneumatic actuator, where real-time regulation of air inflows and outflows via force compliance control maintains a constant, predefined force after the impact phase, independent of the stroke position. Comparisons of contact forces between force controlled robots and those with Active Contact Flanges are addressed in e.g. [2, 6]. The setup with the ACF outperforms the force controlled robots in quality, speed and accuracy. An overview about robotic end-effectors for manufacturing, where various methods are compared, can be found in [5]. Contact forces between robots and the environment are also important for human robot collaboration. Maximum forces for safe collaborations are defined in [3]. A machine learning approach for such safe impact situations in human-robot interactions can be found in e.g. [4]. This work provides an analytical formula to determine the maximum contact force of an ACF during the impact phase and can later be used for training neural networks addressing such collaboration tasks.

The Third Austrian Symposium on AI, Robotics, and Vision (AIROV26).

2 Dynamical Model

The considered setup of the system under consideration is shown in Fig. 1. The left side shows a picture of the floor mounted ACF, without the robotic system visible. To determine the real contact forces, a force sensor is mounted on an external robot that contacts the ACF with different speeds. The center sketch illustrates the setup for the dynamical modeling in the absence of robot contact. The analytic model of the ACF is a combination of a spring with spring constant k_F and a damper with damping constant d_F resembling a force controlled pneumatic device. It actuates the mass m_F. An additional serial spring (k_C) is used for the contact model. The robot with the mounted force sensor moves in vertical z direction within the base frame $\mathcal{F}_I$ of the robotic system with position $\mathbf{r}_E$ and velocity $\mathbf{v}_E$ and gets in contact with the ACF at fixed position $\mathbf{r}_0$, which is the reference position for following considerations where the ACF is at its maximum stroke. It has to be mentioned, that only the z component with respect to base frame $\mathcal{F}_I$ of the end-effector motion $(r_{E,z}, v_{E,z}, r_{0,z})$, but represented in modeling frame $\mathcal{F}_M$, is of interest for spring compression. The right view in Fig. 1 depicts a schematic of the robot in contact with the already partially compressed ACF, which leads to a deformation $s = x(t) - (r_{E,z}(t) - r_{0,z})$ of the modeled contact spring depending on the position of the grinding pad $(r_{E,z}(t) - r_{0,z})$ and position $x(t)$ of mass m_F in modeling frame $\mathcal{F}_M$.

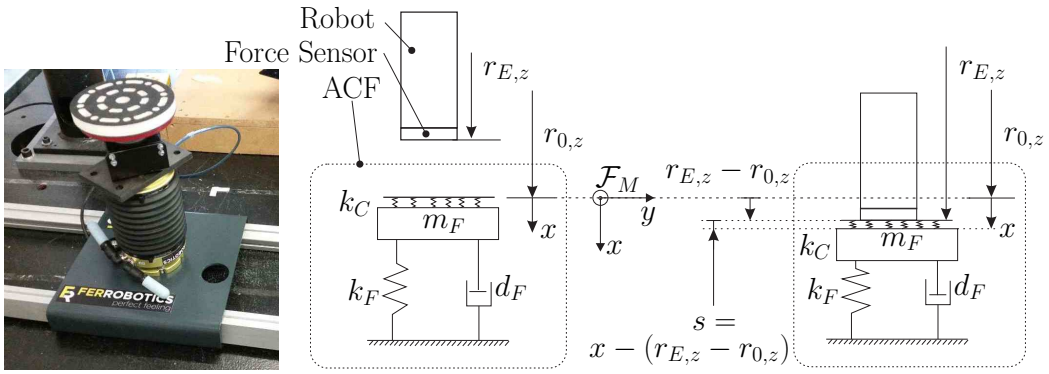

Figure 1: (l) Active Contact Flange with grinding pad in test environment in absence of robot, (m) Schematic of setup before contact, (r) Schematic of setup in contact

2.1 Modeling

An evaluation of different contact models (e.g. different parallel/serial springs) yields to the model in Fig. 1. The active contact flange with moving mass m_F consists of a spring (k_F)/damper(d_F) combination in parallel, enhanced by a contact stiffness k_C. The equation of motion (EOM) for this simplified model with x as degree of freedom, defined from the uncompressed ACF position to the position of mass m_F, and neglected gravitation is

$$m_F\ddot{x} + d_F\dot{x} + k_F x = F_C, \quad x(0) = \dot{x}(0) = 0. \tag{1}$$

The contact force F_C is zero as long as no contact appears. In case of contact, this force is defined as $F_C = -k_C(s + s_0)$, with a penetration depth s and a pretension of s_0. Since the contact is established between an external robot at end-effector position $r_{E,z}(t)$ and an ACF, which are getting in contact at position $r_{0,z}$, the expression can be further evaluated to

$$F_C = -k_C(x(t) \underbrace{-r_{E,z}(t) + r_{0,z}}_{-v_{E,z}t} - \frac{F_P}{k_C}) \tag{2}$$

with penetration depth $s = x(t) - (r_{E,z}(t) - r_{0,z})$ as introduced above and pretension $s_0 = -F_P/k_C$ of the contact stiffness. Velocity $v_{E,z}$ represents the contact velocity between the ACF and the robot, which is assumed to be constant during the contact phase and further stated with v_E for simplicity. Time t starts at the moment of contact, where $r_{E,z}$ equals $r_{0,z}$. The constant pretension force F_P is applied to the ACF to hold it on its maximum position. Using the contact force Eq. 2 in the EOM Eq. 1 results in

$$m_F\ddot{x} + d_F\dot{x} + (k_F + k_C)x = k_C v_E t + F_P, \tag{3}$$

which is a linear time invariant differential equation that can be solved analytically.

2.2 Analytic Solution

The solution for the differential equation Eq. 3 can be split in a homogeneous part and a particular part ($x(t) = x_H(t) + x_P(t)$). For the homogeneous solution x_H, the differential equation

$$\ddot{x} + \underbrace{\frac{d_F}{m_F}}_{2\delta} \dot{x} + \underbrace{\frac{k_F + k_C}{m_F}}_{\omega^2} x = 0 \tag{4}$$

is considered, where the solution can be expressed by

$$x_H = e^{-\delta t}(a \cos \nu t + b \sin \nu t), \tag{5}$$

see e.g. [1] for details. Herein, δ is the damping coefficient and $\nu = \sqrt{\omega^2 - \delta^2}$ the frequency, while constants a and b have to be evaluated based on the initial conditions of the overall solution. ω is the frequency of the undamped system.
An Ansatz for the particular solution of Eq. 3 is chosen as

$$x_P = c_0 + c_1 t, \tag{6}$$

with constants c_0 and c_1. Using this Ansatz in the EOM and evaluating the constants (initial conditions $x(0) = 0$, $\dot{x}(0) = 0$) yields the overall solution $x = x_H + x_P$ as

$$x(t) = e^{-\delta t}(a \cos \nu t + b \sin \nu t) + \frac{F_P}{k_F + k_C} + \frac{k_C v_E}{k_F + k_C} t - \frac{d_F k_C}{(k_F + k_C)^2} v_E, \tag{7}$$

where a and b are constants. Note that this solution is only valid a short time after getting in contact. However, in this time interval, the maximum contact force occurs, which makes the solution usable for the evaluation.

2.3 Maximum Contact Force

With the analytic solution Eq. 7 on hand, the contact force can be evaluated as

$$F_C = k_C(v_E t - x) + F_P. \tag{8}$$

Seeking for the maximum value leads to the optimization problem

$$\frac{dF_C}{dt} = 0, \tag{9}$$

that has a general solution of the form

$$A \cos \nu t + B \sin \nu t + C = 0, \tag{10}$$

where A, B and C are constants. This expression can be solved for the time $t = t_{max}$ of maximum contact force, which finally yields to the force

$$F_{C,max} \quad = \quad k_C(v_E t_{max} - x(t_{max})) + F_P. \tag{11}$$

3 Experimental Evaluation

The parameters for a test setup including $m_F, d_F, k_C, ...$ are identified based on force responses for various test cases and are therefore available for the evaluation of the maximum contact force in Eq. 11. An exemplary result for a desired force $F_d = 100$ N and different contact speeds v_E is shown in Tab. 1. The desired force is controlled by the ACF due to the pneumatic actuation. This actuation is much slower than the force response and therefore does not enter the contact force calculation. It can be seen, that the measured and calculated maximum contact forces coincide very well with a maximum relative error of 5 %. Similar results are achieved for different masses, pads and forces F_P. Note, that Tab. 1 additionally includes a value for the maximum contact velocity, in case the maximum applicable force is given by the considered test object that has to be e.g. polished. The maximum force for fragile objects is hereby much lower than for stiff ones, therefore the contact velocity can be lowered to a tolerable value. Figure 2 shows the measured contact forces for the different contact velocities v_E of the test case from Tab. 1.

v_E in m/s	$F_{C,max}$ Model in N	F_C Measurement in N	relative Error in %
0.05	108	110	1.2
0.1	130	137	5
0.2	195	198	1.5
0.3	271	282	4
0.35	310	320	3

Table 1: Maximum contact forces for $F_d = 100$ N.

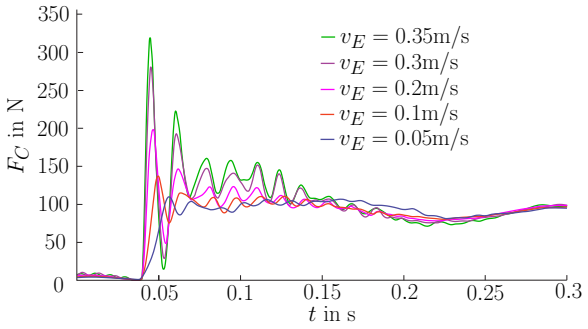

Figure 2: Measured contact forces for $F_d = 100$ N.

4 Conclusion

An analytical solution for the evaluation of maximum contact forces between an object and an Active Contact Flange is presented. The dynamical solution yields to highly accurate results for the contact forces at given contact velocities. Conversely, it can be used to determine the maximum contact velocity resulting from a given maximum contact force. Future work will use the test data to train a neural network that directly evaluates the maximum contact forces.

Acknowledgments and Disclosure of Funding

This work has been supported by the "LCM – K2 Center for Symbiotic Mechatronics" within the framework of the Austrian COMET-K2 program.

References

[1] Hans Dresig. *Schwingungen mechanischer Antriebssysteme: Modellbildung, Berechnung, Analyse, Synthese*. Springer Verlag, 2001.

[2] Stefan Gadringer, Hubert Gattringer, and Andreas Mueller. Assessment of force control for surface finishing – an experimental comparison between universal robots ur10e and ferrobotics active contact flange. *Mechanical Sciences*, 13(1):361–370, 2022.

[3] ISO/TS. Technical specification: Robots and robotic devices: Collaborative robots, standard no. iso/ts 15066:2016. *The International Organization for Standardization, The International Organization for Standardization Technical Specification,*, 2016.

[4] Nemanja Kovinčić, Hubert Gattringer, Andreas Müller, and Mathias Brandstötter. Physics-guided machine learning approach to safe quasi-static impact situations in human–robot collaboration. *Journal of Computational and Nonlinear Dynamics*, 19(7):071011, 2024.

[5] Abdelkhalick Mohammad, Erhui Sun, Junfu Zhou, Guilin Yang, Guolong Zhang, Jokin Munoa, and Asier Barrios. Robotic end-effectors for manufacturing: Recent developments and future research challenges. *International Journal of Machine Tools and Manufacture*, 2026.

[6] Alexander Winkler and Jozef Suchy. Force controlled contour following on unknown objects with an industrial robot. In *IEEE International Symposium on Robotic and Sensors Environments (ROSE)*, page 208–213, 2013.